Strathclyde Engagement with the National HVDC Centre: Development and Validation of Type 3 Turbine Impedance

Doc. Type:	Technical report	*Date:*	***08/09/2021***
Doc. Nº:	**USTRATH-HVDC Centre-P3-002**	*Issue:* ***2***	*Page:* **1** *of* 15
Title:	Development and Validation of Type 3 Turbine Impedance		

	Name&Function	*Signature*	*Date*
Prepared by:	Callum Henderson Lie Xu University of Strathclyde		08/09/2021
Approved by:	Lie Xu University of Strathclyde		09/09/2021
Authorized by:	Ben Marshall The National HVDC Centre		04/11/2021
Accepted by:	Simon Marshall The National HVDC Centre		08/11/2021

DISTRIBUTION LIST	N	A	I
Internal			
External			

N=Number of copy
A=Application
I=Information

TABLE OF CONTENT

1 General introduction

Previous studies have developed small signal admittance models of the MMC and LCC converters, and the methods to use the converter and network admittances to assess system stability. It has shown that different converter systems exhibit different characteristics in their admittances which are also affected by their operating point, control mode and control parameter setting.

The integration of AC connected wind farms into the existing power network has significantly changed the characteristics of the system and adequate small signal wind turbine models will be required to assess system stability considering the existence of difference converter technologies. While the small signal behaviour of Type 4 turbine has been extensively studied, the small signal impedance of doubly-fed induction generator (DFIG) based Type 3 turbine has not been well understood.

The purpose of this study is to develop small signal admittance model of Type 3 turbine under different control modes and operating points. The admittances of Type 3 turbine are then compared to the Type 4 turbine to highlight the main differences between the two. The small-signal admittances of both turbine types from the analytical models are verified against the measurements from time-domain models.

2 Type 3 Wind Turbine System Modelling and Admittance

This section describes the modelling process and obtained impedance for the Type 3 (DFIG) wind turbine system. For comparison, the Type 4 wind turbine using permanent magnet synchronous generator will be briefly introduced in Section 3.

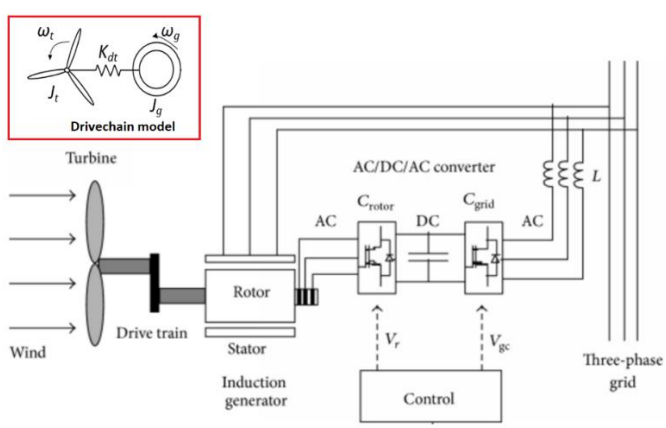

Figure 1 Type 3 turbine diagram

2.1 Type 3 Turbine System

The Type 3 turbine consists of a DFIG with the stator connected directly to the grid. A partially rated back-to-back converter links the rotor to the grid via a filter as shown in Figure 1. A mechanical system containing

a two-mass drivetrain generating the rotor speed is also included in the model. The grid-side converter (GSC) maintains the DC terminal voltage while different control modes can be enabled on the rotor side converter (RSC).

2.2 DFIG Model

The general model of DFIG is well understood so only brief introduction is provided here. The DFIG is modelled in the dq-frame using the following equations:

$$V_{qs} = R_s i_{qs} + \frac{d\phi_{qs}}{dt} + \omega\phi_{ds} \tag{1}$$

$$V_{ds} = R_s i_{ds} + \frac{d\phi_{ds}}{dt} - \omega\phi_{qs} \tag{2}$$

$$V'_{qr} = R'_r i'_{qr} + \frac{d\phi'_{qr}}{dt} + (\omega - \omega_r)\phi'_{dr} \tag{3}$$

$$V'_{dr} = R'_r i'_{dr} + \frac{d\phi'_{dr}}{dt} - (\omega - \omega_r)\phi'_{qr} \tag{4}$$

$$\phi_{qs} = L_s i_{qs} + L_m i'_{qr} \tag{5}$$

$$\phi_{ds} = L_s i_{ds} + L_m i'_{dr} \tag{6}$$

$$\phi'_{qr} = L'_r i'_{qr} + L_m i_{qs} \tag{7}$$

$$\phi'_{dr} = L'_r i'_{dr} + L_m i_{ds} \tag{8}$$

where:

V_{qs} = q-axis stator voltage, V_{ds} = d-axis stator voltage

V'_{qr} = q-axis rotor voltage referred to the stator, V'_{dr} = d-axis rotor voltage referred to the stator

i'_{qr} = q-axis rotor current referred to stator, i'_{dr} = d-axis rotor current referred to stator

i_{qs} = q-axis stator current, i_{ds} = d-axis stator current

ϕ_{qs} = q-axis stator flux, ϕ_{ds} = d-axis stator flux

ϕ'_{qr} = q-axis rotor flux referred to the stator, ϕ'_{dr} = d-axis rotor flux referred to the stator

R_s = stator resistance, R'_r = rotor resistance referred to stator

ω = reference frame rotational speed, ω_r = rotor electrical rotational speed

L_s = stator inductance, L_r = rotor inductor referred to stator, L_m = mutual inductance

2.3 Drivetrain Model

A two-mass drivetrain shown in Figure 1 can be enabled if required and is modelled by the following:

$$\omega_t = \frac{\tau_t - \gamma K_{dt}}{sJ_t} \tag{9}$$

$$\omega_g = \frac{\gamma K_{dt} - \tau_g}{sJ_g} \tag{10}$$

$$\gamma = \frac{\omega_t - \omega_g}{s} \tag{11}$$

where ω_t and ω_g are the turbine and generator rotational speeds respectively. τ_t and τ_g are the turbine and generator torque respectively, while J_t and J_g are the turbine and generator inertias respectively. K_{dt} is the flexible shaft stiffness and γ is the shaft twist angle.

2.4 Converter Control Modes

The Type 3 turbine has a partially rated back-to-back converter where the GSC regulates the DC link voltage and maintains a unity power factor via an internal current loop. The RSC also contains an internal current loop and the outer control algorithm can be changed dependent on goals, such as active power/speed/torque control, reactive power / AC stator voltage control. The following subsections provide diagrams illustrating the different control modes.

2.4.1 Current Control (CC)

No outer-loop is implemented in this control mode with the exception of the GSC DC link voltage controller. A current controller is present on both the rotor and grid side converters with PI controllers used to regulate the d and q-axis current. A GSC DC link controller provides the active power current set-point on the GSC. A PLL is also used for the GSC as shown in Figure 2.

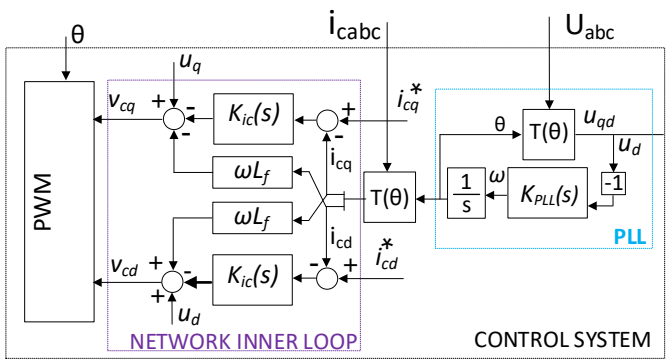

Figure 2 Current controller layout

2.4.2 Active Power and AC Voltage Control (PV)

In active power and AC voltage control, a PI controller regulates the active power by providing the active current command, and a voltage droop is also applied to provide reactive current command. Figure 3 shows the control diagrams for the RSC, where K_U represents the voltage droop gain.

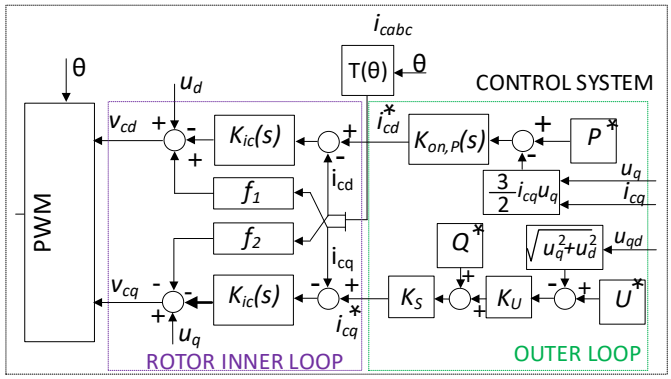

Figure 3 Type 3 RSC PV controller

2.4.3 Speed and AC Voltage Control (WV)

In speed control the rotor speed is maintained via a PI controller on the RSC active power axis. However, in this mode, the AC voltage droop used in PV control is replaced with PIs to maintain a constant PCC voltage. Figure 4 shows the control diagram for the RSC of the Type 3 turbine, where a PI controller is used for AC voltage control in the RSC. As seen, the active power controller in Figure 3 is replaced with a speed controller on the machine side, which follows a command from a MPPT algorithm or turbine master controller. In these cases the speed command from the MPPT is assumed constant for the given parameter set.

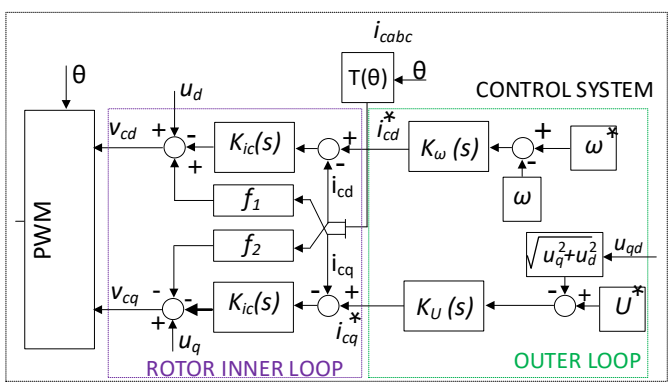

Figure 4 Type 3 RSC WV controller

2.5 Small-Signal Admittance

The small-signal model is constructed using the equations detailed in the previous sections. The model is linearised at different operating points. To extract the small-signal admittance a distbance is injected in the dq-frame PCC voltage and the resulted converter current is measured giving:

$$Y_c(s) = \frac{\delta I_c(s)}{\delta V_{PCC}(s)} \tag{12}$$

where $Y_c(s)$ is the converter admittance, $I_c(s)$ is the converter current and $V_{PCC}(s)$ is the PCC voltage. The dq admittance is then transformed into the pn-frame.

It is necessary to note that for Type 3 turbine, the AC admittance is the combined admittance of the DFIG stator terminal and the GSC terminal.

2.6 Admittance Results

This section presents the results from analysis conducted using the Type 3 turbine model rated at 5 MW. For reference, the three control modes for the DFIG RSC are current control (CC), power and AC voltage control using droop (PV), and speed control with AC voltage control using PI regulator (WV). As previously described, for the GSC of the DFIG system, it controls the common DC link voltage with a zero reactive power order. The pn-admittance is compared for each control mode applied to the Type 3 turbine in Figure 5.

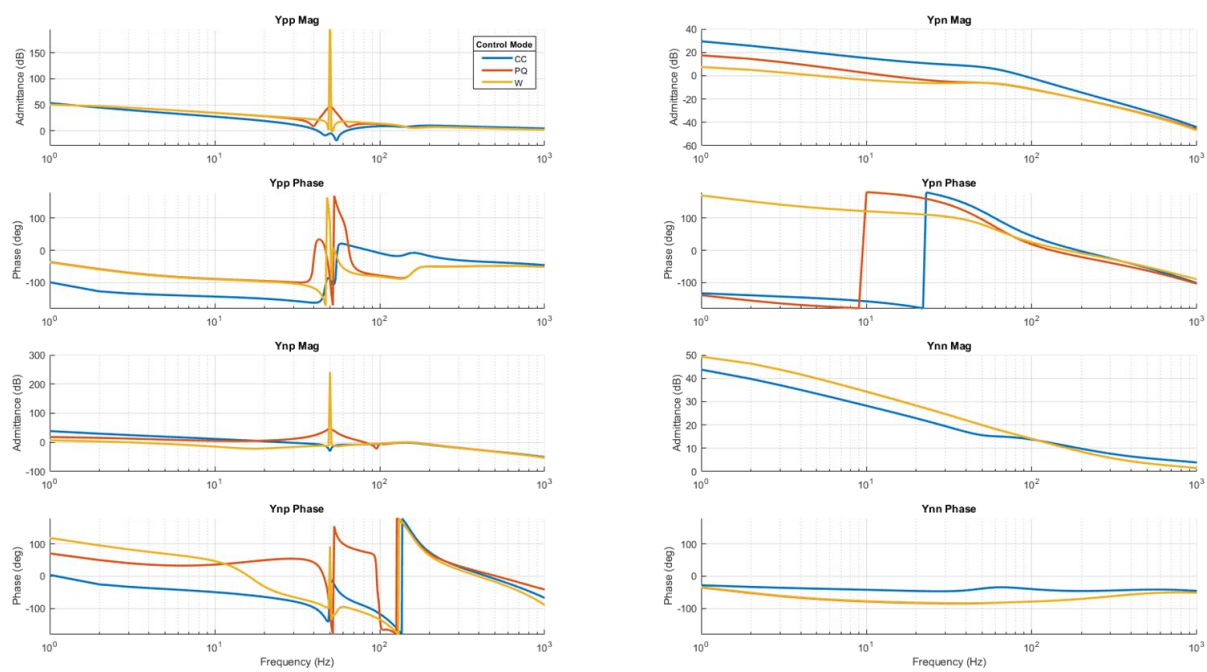

Figure 5 PN admittance of Type 3 turbine with different control modes

As seen from Figure 5, the control modes form similar admittance traces largely due to the common current loop in each controller. The coupling from negative to positive sequence is larger without an outer loop controller. The highest damping (lowest admittance) around 50 Hz in the positive sequence is achieved with current control and further outer loop control goals reduce the damping and stability of the system. For the WV mode, the PI regulator used for the AC voltage control produces a large spike at 50Hz (i.e., very high admittance / low impedance at 50Hz since the AC voltage is largely kept constant by the PI controller). Current control (CC) offers a larger region of negative damping (where the phase (ϕ) satisfies

$90° < \phi \; or \; \phi < -90°$), so needs to be closely assessed for potential negative impact on system stability in these frequency regions.

3 Type 4 Wind Turbine System Modelling and Admittance

This section briefly introduces the modelling process and obtained admittance for the Type 4 wind turbine system.

3.1 Type 4 Turbine system

The Type 4 turbine is represented by a permanent magnet synchronous machine (PMSG) connected to the grid through a fully rated converter and RL filter, as shown in Figure . Similar to the Type 3 turbine, a two-mass drivetrain can be enabled. The GSC regulates the DC link voltage and further control goals can be added to both the machine side converter (MSC) and GSC.

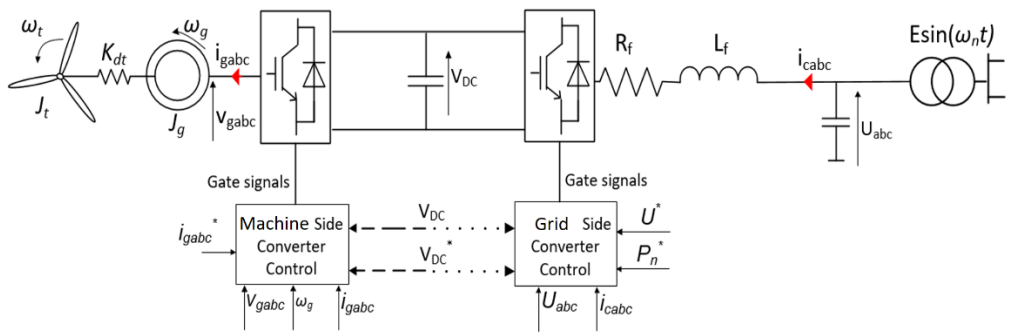

Figure 6 Type 4 turbine diagram

3.2 Permanent Magnet Synchronous Generator and Drivechain Models

The PMSG is also modelled in the dq-frame using:

$$V_{qs} = R_s i_{qs} + \frac{di_{qs}}{dt} L - p\omega_m L i_{ds} - \lambda p \omega_m \tag{13}$$

$$V_{ds} = R_s i_{ds} + \frac{di_{ds}}{dt} L + p\omega_m L i_{qs} \tag{14}$$

$$T_e = 1.5 p \lambda i_{qs} \tag{15}$$

where:

V_{qs} = q-axis stator voltage, V_{ds} = d-axis stator voltage

i_{qs} = q-axis stator current, i_{ds} = d-axis stator current

R_s = stator resistance, L_s = stator inductance, p = pole pairs,

ω_m = generator mechanical speed, T_e = electromagnetic torque, λ = magnetic flux per pole

A two-mass drivetrain model of Type 4 turbine can be represented in a similar way as for Type 3 turbine in Section 2.3. The inertias and shaft stiffness are different for each turbine type due to the different machine speeds and the addition of a gearbox for Type 3.

3.3 Converter Control Modes

For the Type 4 turbine, a fully-rated back-to-back converter is used where the DC link voltage is regulated by the GSC. Since the machine is decoupled from the grid, any PCC voltage control goals must be achieved by the GSC in a Type 4 turbine (while in Type 3, it is mainly achieved by the RSC). Active power control goals are accomplished via outer loop control on the MSC. The following subsections provide diagrams illustrating the different control modes.

3.3.1 Current Control (CC)

No outer-loop is implemented in this control mode with the exception of the GSC DC link voltage controller. A current controller is present on both the machine and grid side converters with PI controllers used to regulate the d and q-axis current. A GSC DC link controller provides the active power current set-point on the GSC. A PLL is also used for the GSC as shown in Figure 7.

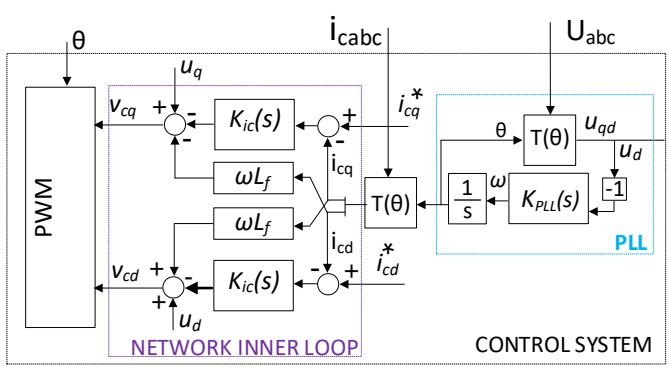

Figure 7 Current controller layout

3.3.2 Active Power and AC Voltage Control (PV)

In active power and AC voltage control, a PI controller regulates the active power by providing the active current command for the MSC, while a voltage droop is applied to the GSC to provide reactive current command. Figure 8 shows the control diagrams for the GSC of Type 4 controllers, where K_U represents the voltage droop gain. As seen in Figure , AC voltage control in Type 4 turbine is applied to the GSC while the machine side controller for Type 4 is the same as the Type 3 shown in Figure 8 without the outer voltage droop loop.

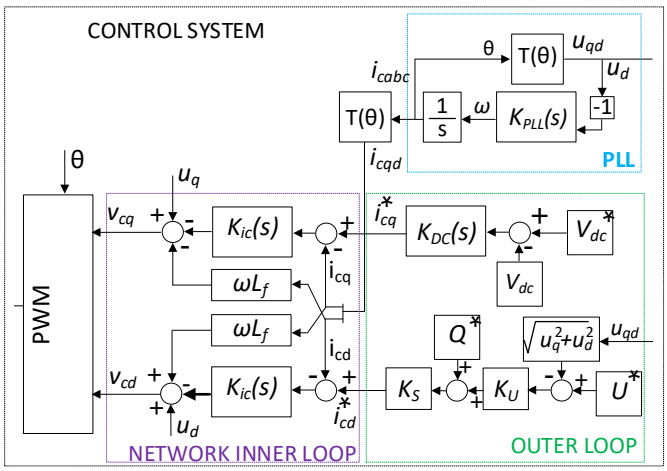

Figure 8 Type 4 GSC PV controller

3.3.3 Speed and AC Voltage Control (WV)

In speed control the rotor speed is maintained via a PI controller on MSC active power axis for Type 4 turbine. However, in this mode, the AC voltage droops used in GSC PV control are replaced with PIs to maintain a constant PCC voltage in a similar way as the RSC of Type 3 turbine shown in Figure 4. The active power controller is replaced with a speed controller on the machine side, which follows a command from a MPPT algorithm or turbine master controller. In the following studies, the speed command from the MPPT is assumed constant for the given parameter set.

3.4 Admittance Results

The admittance of a 5 MW Type 4 turbine is obtained in a similar way as that for Type 3. It is necessary to note that for Type 4, the presented admittence is seen at the GSC terminal.

The pn-admittances of a Type 4 turbine under the three control modes, i.e., CC, PV, and WV, are shown in Figure 9. As seen, PV control provides the highest admittance and least damping across the frequency range while WV control exhibits the least coupling between the positive and negative sequence similar to the Type 3 turbine. Large regions of negative damping occur for CC at low frequencies and at high frequencies for PV control. Overall, PV control appears to be the least stable operating mode though the exact impact of the control mode needs to be considered for specific network condition. Similar to Type 3 turbine, the positive spike at 50Hz with WV mode is due to the use of PI controller in the AC voltage regulation.

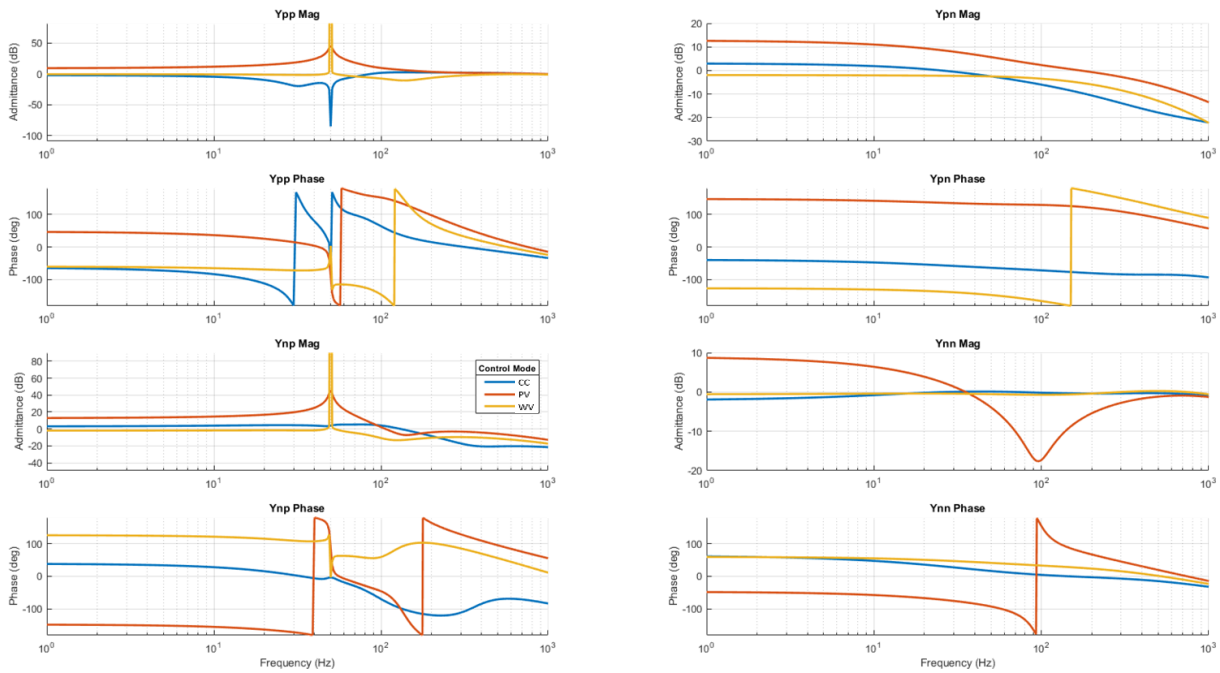

Figure 9 PN admittance of Type 4 turbine with different control modes

4 Comparisons of Type 3 and Type 4 Turbines

In this section, the admittances of the two types of turbines are compared considering the different control modes, and active and reactive power operating points.

4.1 CC Control Mode

The admittances of the Type 3 and Type 4 turbines with CC at 0 p.u. and 1 p.u. active power are compared in Figure and Figure , respectively. As seen from Figure , the Type 3 turbine provides lower damping (higher admittance) in CC mode for both the positive and negative sequence admittance. In addition, the sequence coupling is larger for the Type 3. At high frequencies, the difference between Type 3 and Type 4 is small.

The Y_{pp} admittance in Figure 10 also shows a negative spike at 50 Hz for Type 4 Turbine. This is due to the fact that the current variation at 50 Hz is limited by the current controller during a voltage disturbance resulting in low admittance (i.e., small $\Delta I/\Delta V$). In comparison, the Y_{pp} admittance for Type 3 turbine under does not have such a negative spike. This is largely due to the fact that the admittance of a Type 3 turbine is the sum of the admittances of the DFIG stator and the GSC, while the characteristic of the GSC in Type 3 WT which controls the DC voltage does not have the same feature as CC of the stator (via RSC).

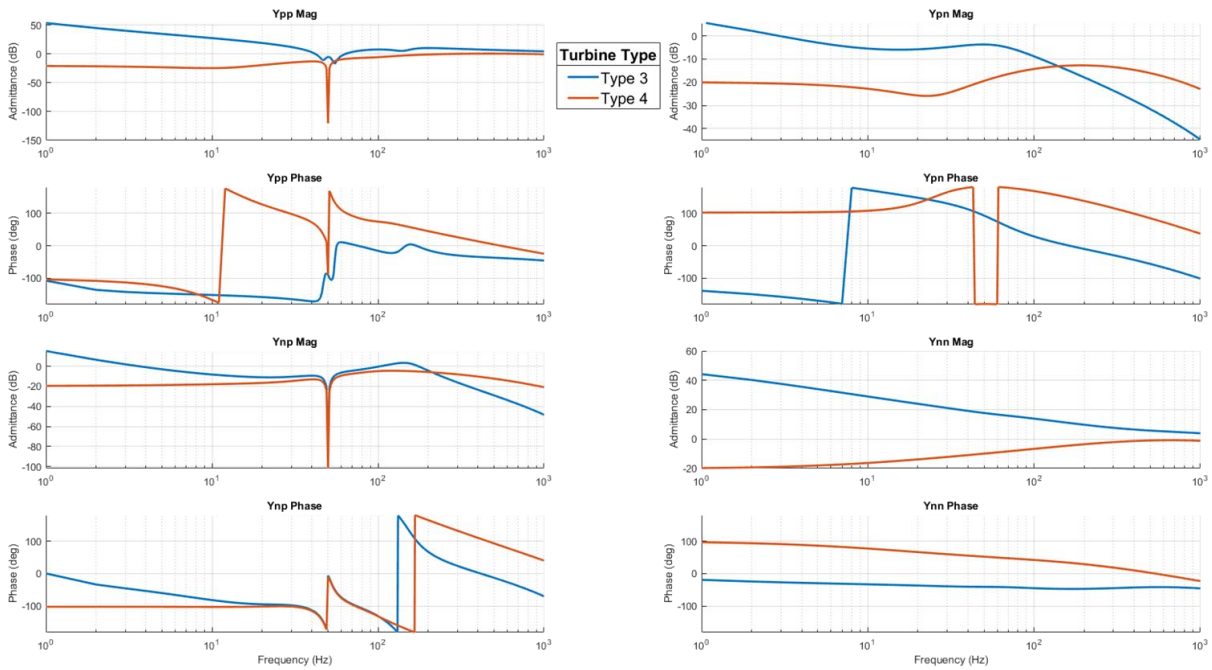

Figure 10 Comparison of Type 3 and Type 4 turbine under CC at P = 0 p.u.

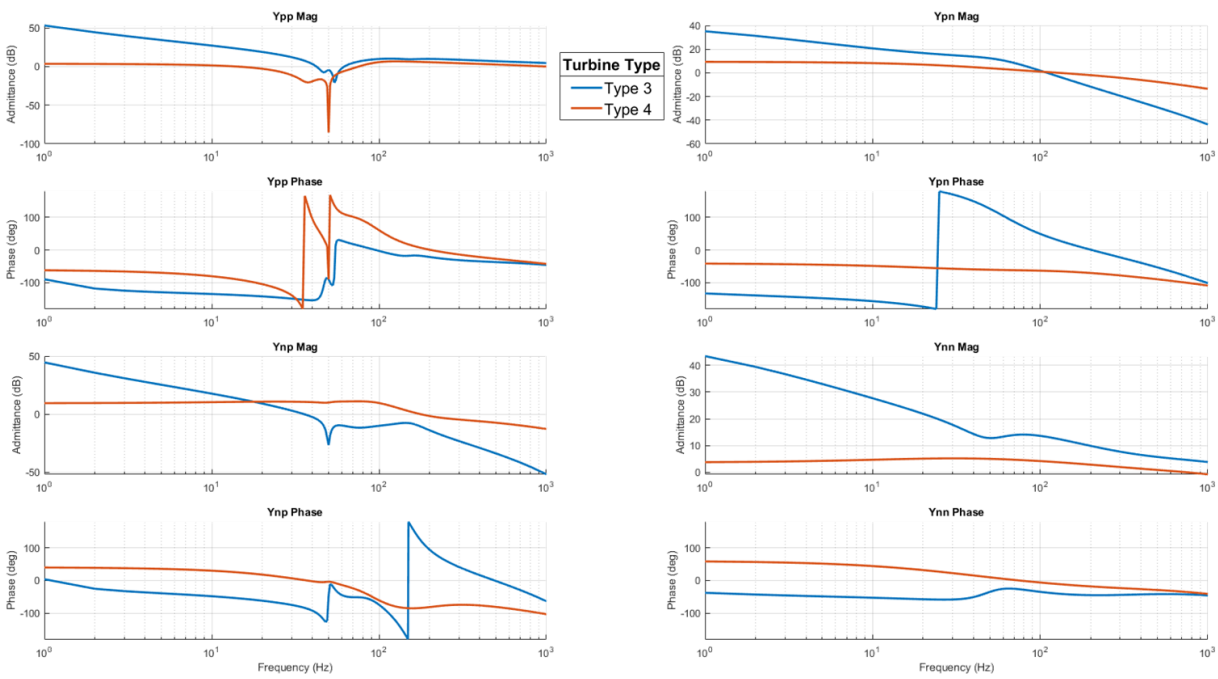

Figure 11 Comparison of Type 3 and Type 4 turbine under CC at P = 1 p.u.

Comparing Figure 1, it is seen that Type 4 turbine is more susceptible to operating point change. The damping is significantly reduced at higher active power. However, the admittance for the Type 3 exhibits no real change at different operating points, as it always has a higher admittance and lower damping. Thus,

stability of Type 4 turbine system may be more challenging as the large changes in admittance places more stringent conditions on the grid impedance to avoid unwanted interactions and maintain stability.

4.2 PV Control Mode

In PV control mode a reactive power set-point is also present to facilitate the support of the PCC voltage. Figure shows the admittance for 0 p.u. active and 0 p.u. reactive power, Figure contains traces for 1 p.u. active and 0.5 p.u. reactive power, and Figure illustrates the admittance for 1 p.u. active and -0.5 p.u. reactive power set-points.

From Figure , the admittance is much larger for the Type 3 turbine providing lower network damping at low frequencies. However, both types appear to have very similar admittance at 50 Hz due to the same droop constant used in the AC voltage droop controller. The Type 3 has a collection of poles and zeros around 50 Hz which results in the strange shape. Unlike CC mode the coupling between sequences is larger for the Type 4 turbine.

From Figure 13, the operating point has a much smaller effect on the Type 4 turbine in PV mode than in CC mode. The traces for both turbines are largely the same with only a small difference between 50 and 200 Hz. Regions of negative damping are smaller for the Type 3 turbine and the Type 4 turbine continues to exhibit the highest sequence coupling. From Figure , the reactive power set-point can be seen to have little effect on the output admittance as the traces are almost identical to Figure .

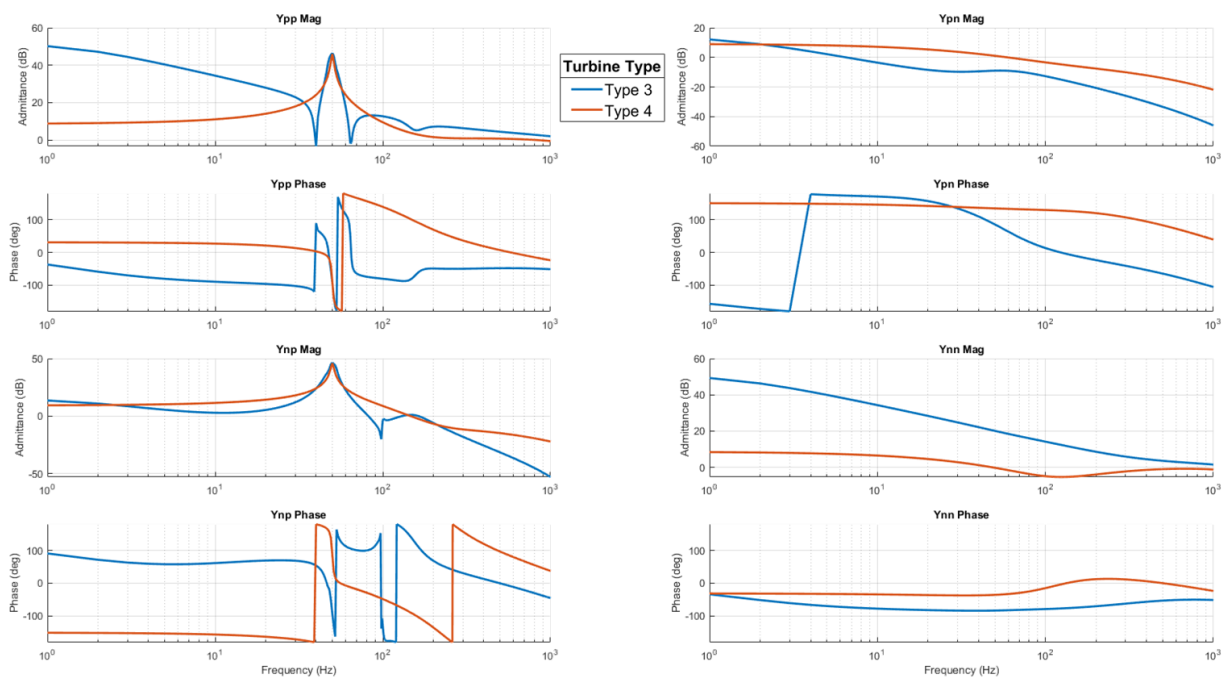

Figure 12 Comparison of Type 3 and Type 4 turbine under PV control with P = 0 p.u, Q = 0 p.u.

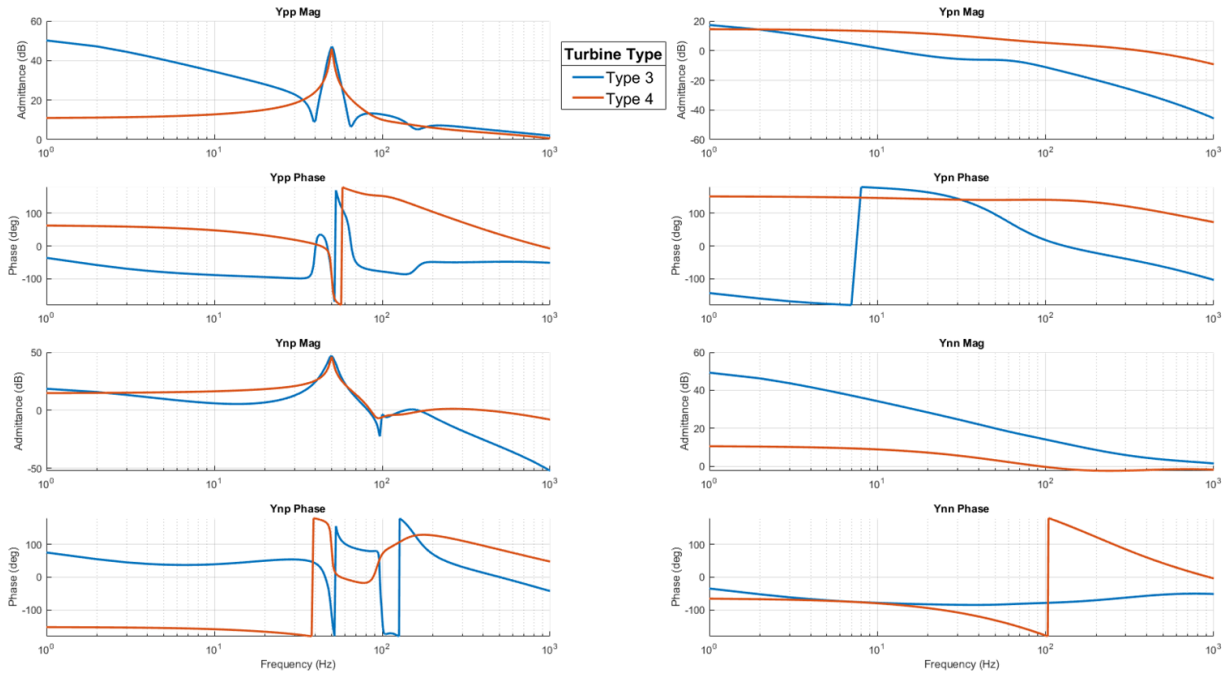

Figure 13 Comparison of Type 3 and Type 4 turbine under PV control at P = 1 p.u, Q = 0.5 p.u.

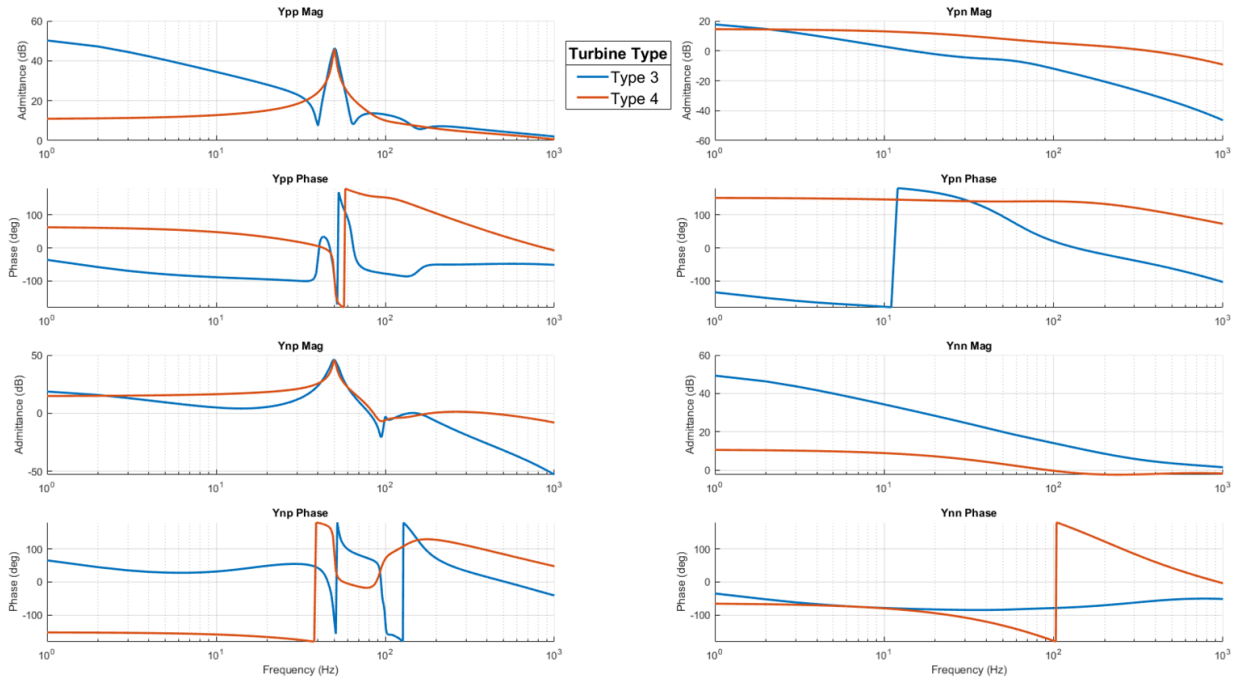

Figure 14 Comparison of Type 3 and Type 4 turbine under PV control at P = 1 p.u, Q = -0.5 p.u.

4.3 WV Control Mode

In speed and AC voltage control mode, only a rotor speed set-point is used while the AC voltage control (PI) automatically regulates the PCC voltage. Figure shows the admittance at 0.96 p.u. speed and Figure provides the traces for 1.04 p.u. speed.

From Figure , the negative sequence admittance for the Type 4 turbine is the lowest in speed control mode indicating the highest network damping. The positive sequence admittance is also the smallest when considering cases where power is being transferred. The sequence coupling is lower for Type 4 turbines than Type 3 under speed control. Spikes at 50 Hz in the positive sequence are observed for both turbines due to the integral AC voltage control.

From Figure , similar to PV control the operating point has a smaller effect on the Type 4 turbine when in speed control. The same occurs for Type 3. However, at higher speeds the sequence coupling appears to be lower for the Type 3 turbine but remains constant for Type 4.

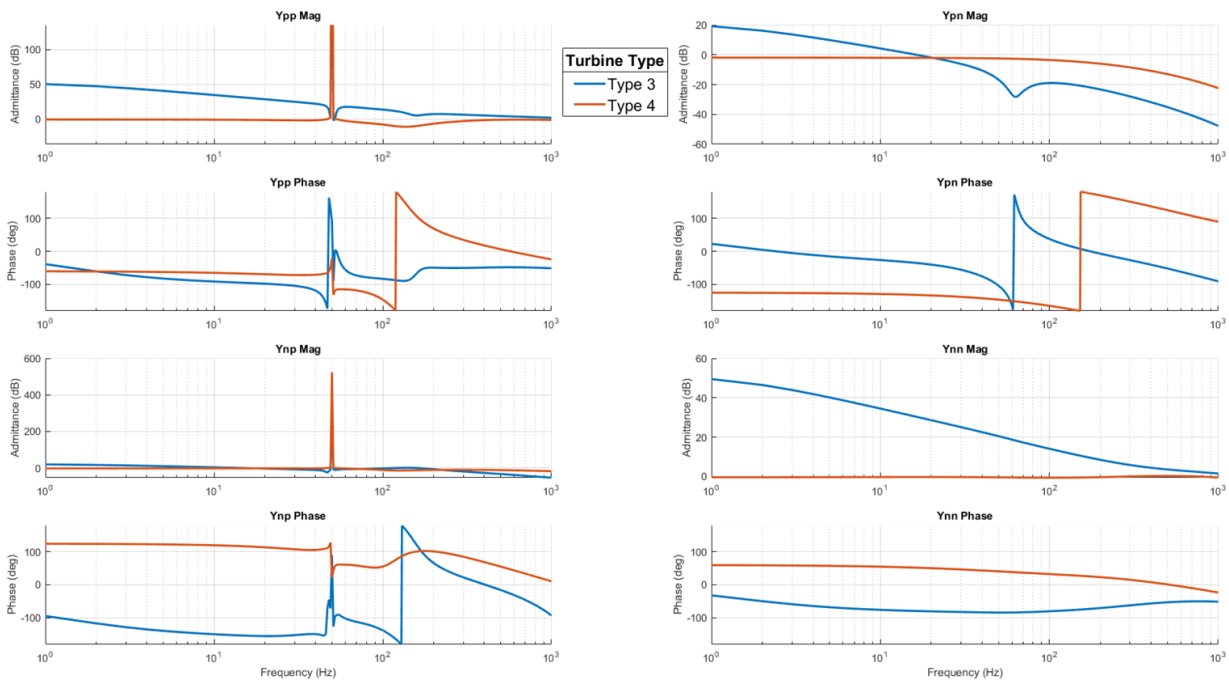

Figure 15 Comparison of Type 3 and Type 4 turbine for WV at 0.96 p.u. speed

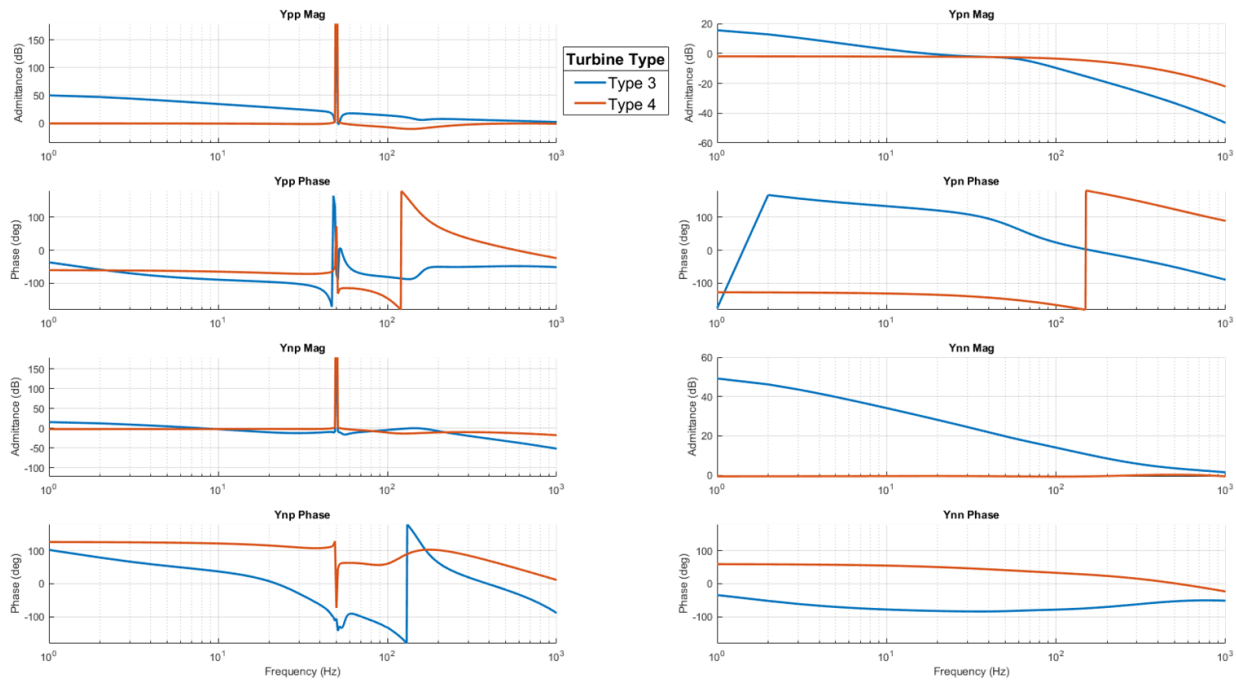

Figure 16 Comparison of Type 3 and Type 4 turbine for WV at 1.04 p.u. speed

5 Conclusions

The modelling procedure for both Type 3 and Type 4 wind turbine systems has been presented. Different control modes including current control (CC), active power and AC voltage droop control (PV) and speed and AC voltage PI control (WV) have been analysed. It is necessary to note that the admittance of Type 3 turbine contains sum of the admittances of the DFIG stator terminal and the GSC so both need to be considered. Analysis confirms that:

- CC mode offers the lowest admittance and highest damping indicating the most stable approach. However, the Type 4 turbine admittance is highly sensitive to operating point changes while in current control mode.
- For the Type 4 turbine PV control which is commonly adopted in wind farms in GB gives the highest admittance and lowest damping, while both PV and WV are similar for the Type 3 considering the entire frequency range.
- Overall, the Type 4 turbine offers a much lower admittance and higher damping at all operating points for all control modes. This suggests that Type 4 turbines may suit a stronger grid connection while Type 3 could operate better for weaker connections.

While the differences between Type 3 and Type 4 turbines under a given operating condition can be seen from the analysis presented, it should be noted that converter admittance is highly variable and dependent on numerous physical and control parameters. Hence, it is challenging to make stability conclusions based on a single admittance plot. Most systems are not unstable when analysed individually. In order to

adequately determine system stability, the admittances must be combined with other network components as the interactions between components is usually where stability issues arise.